



iJRASET

International Journal For Research in
Applied Science and Engineering Technology



INTERNATIONAL JOURNAL FOR RESEARCH

IN APPLIED SCIENCE & ENGINEERING TECHNOLOGY

Volume: 11 Issue: VIII Month of publication: Aug 2023

DOI: <https://doi.org/10.22214/ijraset.2023.55107>

www.ijraset.com

Call:  08813907089

E-mail ID: ijraset@gmail.com

Research on Square and Circular Steel Tubular Columns with Deconstructable Splice Joint Under Cyclic and Axial Testing

Nehana V. G¹, Prof. Krishnachandran V.N²

¹APJ Abdul Kalam Technological University, M Tech Student, Department of Civil Engineering-Structural, NSS College of Engineering, Palakkad, 678001 Kerala, India,

²Assistant Professor, Department of Civil Engineering, NSS College of Engineering, Palakkad, 678001, Kerala, India

Abstract: A steel tubular column is a vertical structural member used in construction to provide essential support. Splice joint is a method of joining two members end to end. When the material being joined cannot be obtained in the desired length, the splice joint is used. For high rise buildings the continuity of columns may break, hence splice connections are provided and columns are installed. Splice joints are deconstructable type joints as the failed parts can be repaired, reassembled or can be even removed when failure occurs. These papers focuses on developing models of square and circular cross sections of steel tubular columns with deconstructable splice joint using a finite element software ANSYS and study their structural behavior. This paper includes a parametric study on the effect of axial loading by varying splice length and thickness, bolt diameter and pattern of square and circular cross sections of steel tubular columns with deconstructable splice joints. Bending moment rotation curves were obtained from cyclic load testing for square and circular cross sections.

Keywords: Deconstructable splice joint, local buckling, steel tubular columns

I. INTRODUCTION

In addition to the benefits of high construction efficiency, good construction quality, and sustainable development associated with prefabricated steel structures, deconstructable steel structure systems enables quick disassembly and reuse of structural members following the completion of the structure. Deconstructable steel systems therefore have greater promise in the engineering field [4]. Splicing joint is made of lower square steel tubular column, upper column, four numbers of splice plates and number of high strength bolts. The splice plates are designed as four numbers of independent plates in order to make sure that the splice plates well fit into the four other component plates of the column. Steel tubular constructions with distinct advantages are being employed more frequently as long span skyscrapers and high-rise buildings continue to emerge [12]. Deconstructable structural design also refers to the use of reusable materials in the design stage to create structural components that are simple to assemble and disassemble [11]. At present the research on deconstructable steel structure system is very limited. While closed section column-to-column splicing joints frequently use fully welded connections, which can't satisfy the requirements of convenient disassembly, the majority of the column-to-column joints use fully bolted connections [4]. The current study proposes square and circular cross sections of steel tubular column with conventional high-strength bolts in order to realize deconstructable connection of closed section steel column splicing joints. 3-D finite element model was built using Ansys software and further validated against the experiments, which may serve as an important reference for its use in real-world engineering applications. In cyclic loading tests, the bending moment rotation curves were obtained. Axial loadings were given to square and circular column sections and corresponding ultimate load and deflection curves were plotted.

II. VALIDATION

The material properties and dimension for validation is taken from work by Fan.et.al (2022) [4] as shown in Table 1 and Table 2. Specimen H1 is chose for validation were splice connection is exactly placed at middle position. The square steel tubular column of size 2245mmx220mmx10mm is taken for validation. The type of bolt is M24 10.9 grade bolt and number of bolt is 64. The splice plate of size 785mmx168mmx14mm is used. Boundary condition adopted is bottom fixed and top cyclic load acting. Element type used is SOLID 186(steel plates). Connector elements used is BEAM 188(Bolt). Minimum element size is 12mm. Element shape of meshing is HEXAHERDON. Total deformation, equivalent plastic strain and directional deformation is obtained after analysis using ANSYS workbench 2022 R2.

Table 1
Material properties of steel column.

Properties	Value	Unit
Young's modulus	219000	MPa
Poisson's ratio	0.3	
Friction coefficient	0.4	
Yield strength	385.2	MPa

Table 2
Material properties of splice plate.

Properties	Value	Unit
Young's modulus	210000	MPa
Poisson's ratio	0.3	
Yield strength	405.2	MPa

A. Cyclic Loading

Loading is applied as per FEMA protocol enlisted in Table 3. As per this protocol 0.375% of drift is given first. Above 4% if a structure withstand the load without fail, then the structure is said to be seismically best suited. Hence there is no need to test above 4%. Loading Height = $6.9 / 0.00375 = 1840$ mm.

Table 3
Cyclic loading scheme.

Load step	Loading displacement(mm)	Cycle number	Storey drift angle(rad)
1	6.9	6	0.00375
2	9.2	6	0.005
3	13.6	6	0.0075
4	18.5	4	0.01
5	27.7	2	0.015
6	36.9	2	0.02
7	55.4	2	0.03
8	73.8	2	0.04

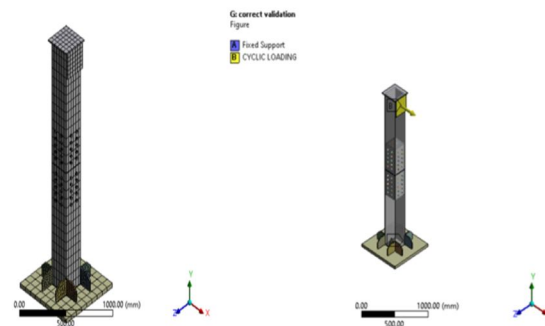


Fig .1. Mmesh and boundary condition applied

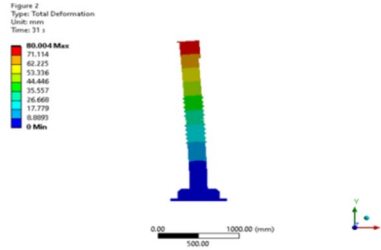


Fig .2. Total deformation

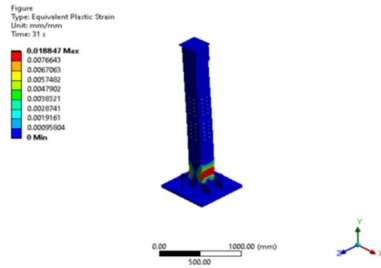
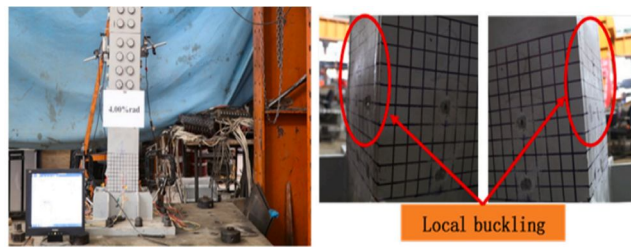


Fig .3. Equivalent plastic strain



(a) specimen H-1.

Fig .4. Failure pattern of local buckling from experiment

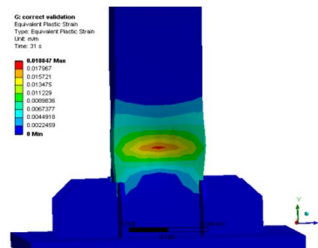


Fig .5. Failure pattern of local buckling after validation from Ansys

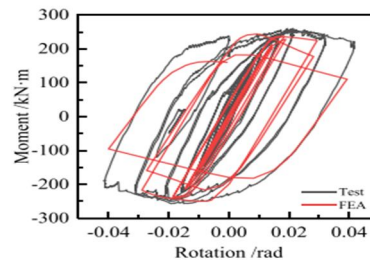


Fig .6. Hysteresis curve obtained from experiment

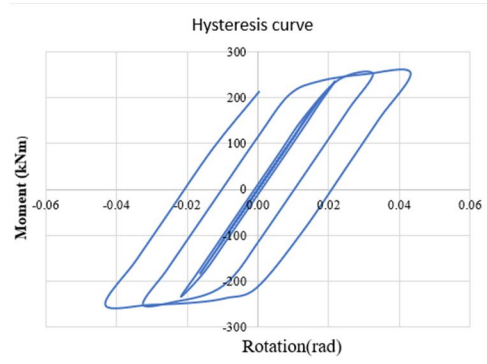


Fig .7. Hysteresis curve obtained from Ansys software after validation

Table 4
Validation results.

	Moment(kNm)	Storey drift(% rad)
EXPERIMENTAL (Base Journal)	253.9	4
FEA	251.77	4.1
% error	0.85	2.44

The ultimate load carrying capacity of the structure from the literature is 3352kN [4] and ultimate load carrying capacity from the validation model is 3561.2kN. The percentage error was found to be 6.34% .hence model is validated.

III. MODELLING AND ANALYSIS OF SQUARE STEEL TUBULAR COLUMN WITH DECONSTRUCTABLE SPLICE JOINT

The square steel tubular column with deconstructable splice joint modeled for validation is taken and tested for axial loading and studied their failure pattern. Bottom hinged and top load is applied.

A. Effect of axial loading by varying thickness of splice plate

Table 5 Cases for varying thickness.

Thickness of splice plate	Designation
14mm	SQUARE AL T14
12mm	SQUARE AL T12
10mm	SQUARE AL T10
8mm	SQUARE AL T8
6mm	SQUARE AL T6

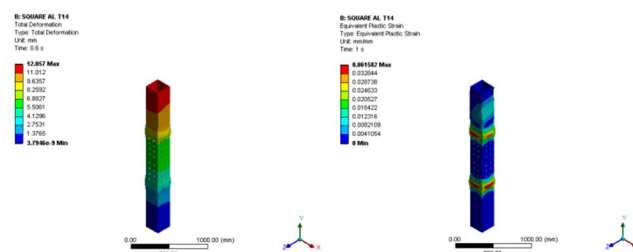


Fig .8. Total deformation and equivalent plastic strain of 14mm splice plate

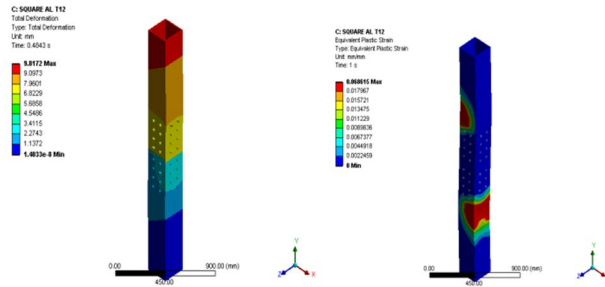


Fig .9. Total deformation and equivalent plastic strain of 12mm splice plate

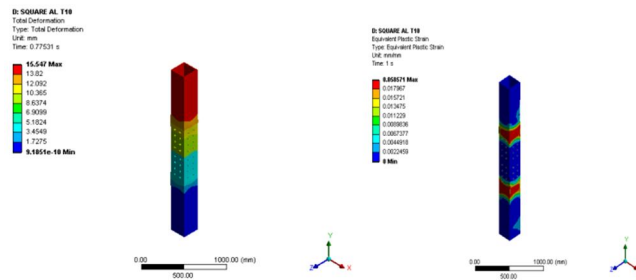


Fig .10. Total deformation and equivalent plastic strain of 10mm splice plate

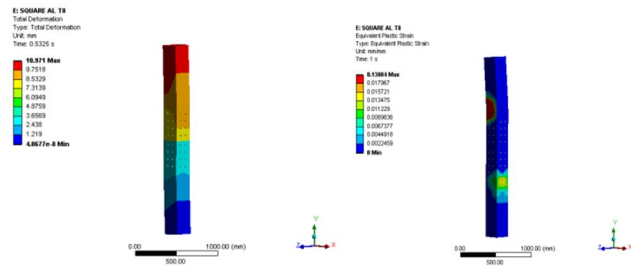


Fig .11. Total deformation and equivalent plastic strain of 8mm splice plate

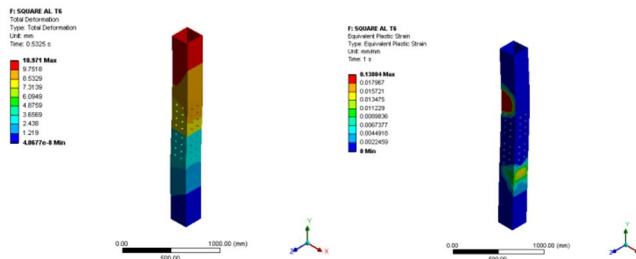


Fig .12. Total deformation and equivalent plastic strain of 6mm splice plate

B. Effect of axial loading by varying length of splice plate

Table 6
Cases for varying length.

Length of splice plate	Designation
785mm	SQUARE AL 785
685mm	SQUARE AL 685
585mm	SQUARE AL 585

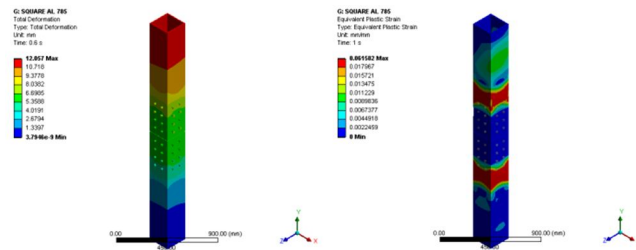


Fig .13. Total deformation and equivalent plastic strain of splice plate of length 785mm

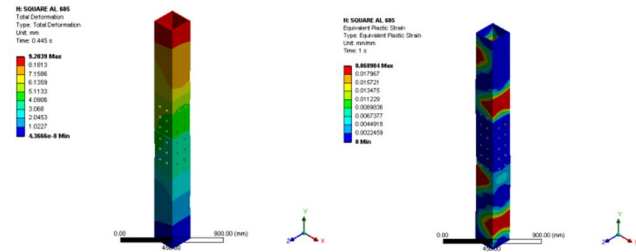


Fig .14. Total deformation and equivalent plastic strain of splice plate of length 685mm

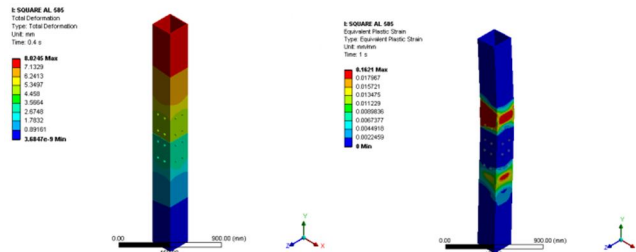


Fig 15: Total deformation and equivalent plastic strain of splice plate of length 585mm

C. Effect of axial loading by varying diameter of Bolt

Table 7
Cases for varying bolt diameter.

Diameter of bolt	Designation
M24	SQUARE AL M24
M22	SQUARE AL M22
M20	SQUARE AL M20
M18	SQUARE AL M18
M16	SQUARE AL M16

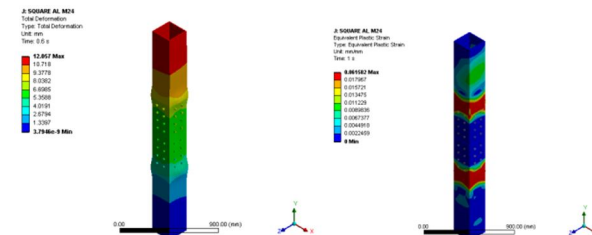


Fig .16. Total deformation and equivalent plastic strain of bolt diameter M24

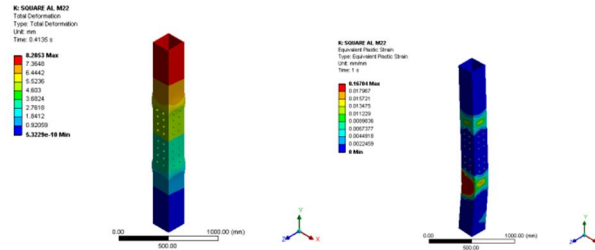


Fig .17. Total deformation and equivalent plastic strain of bolt diameter M22

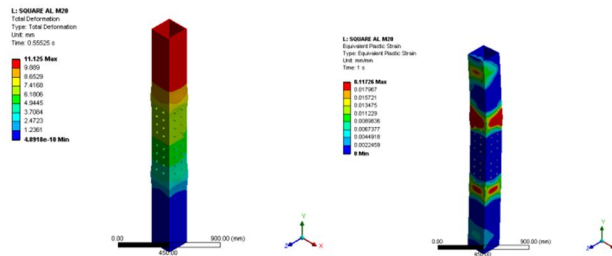


Fig .16.Total deformation and equivalent plastic strain of bolt diameter M20

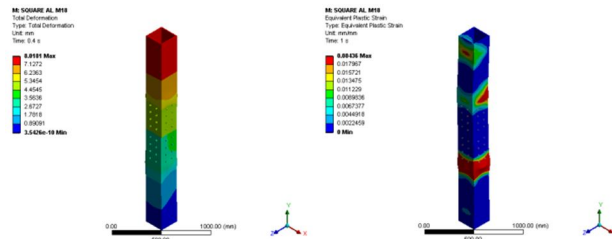


Fig .17. Total deformation and equivalent plastic strain of bolt diameter M18

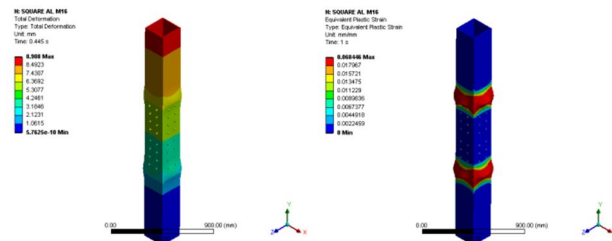


Fig . 18. Total deformation and equivalent plastic strain of bolt diameter M16

D. Effect of Axial Loading by Varying bolt Pattern

Table 8
Cases for varying bolt pattern.

Bolt pattern	Designation
64 bolts	SQUARE AL 64
48 bolts	SQUARE AL 48
32 bolts	SQUARE AL 32

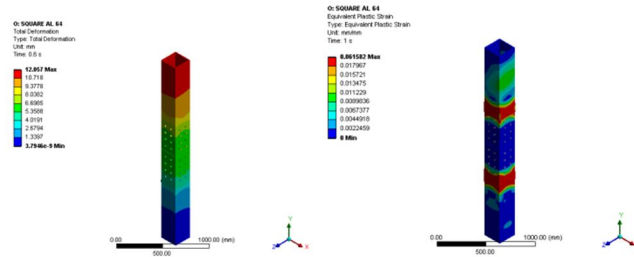


Fig .19. Total deformation and equivalent plastic strain of 64 number of bolts

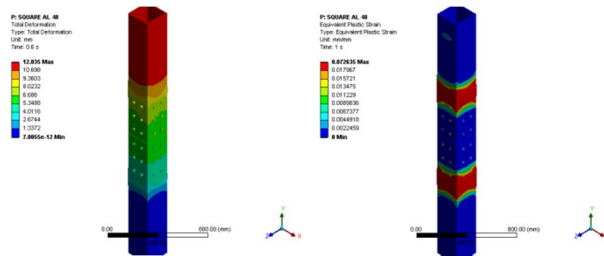


Fig .20. Total deformation and equivalent plastic strain of 48 number of bolts

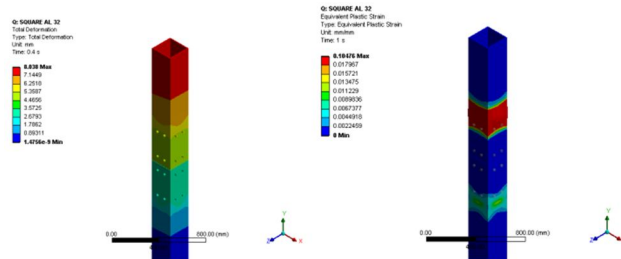


Fig .21. Total deformation and equivalent plastic strain of 32 number of bolts

IV. MODELING AND ANALYSIS OF ELLIPTICAL STEEL TUBULAR COLUMN WITH DECONSTRUCTABLE SPLICE JOINT

Circular steel tubular column with deconstructable splice joint is modeled using square steel tubular as base model. Area of steel is 8424mm^2 . Diameter is 103.56mm. Material properties of column and splice plate are similar to square steel tubular column. For axial testing bottom hinged and top load applied.

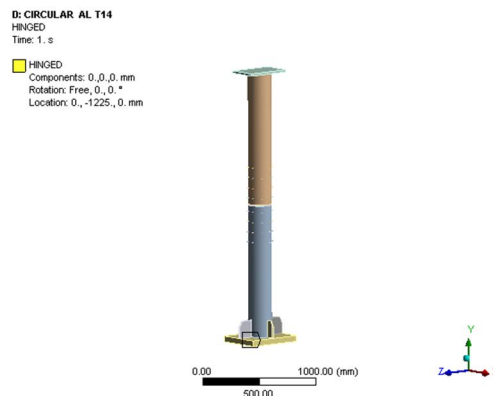


Fig .22. Boundary condition for axial testing

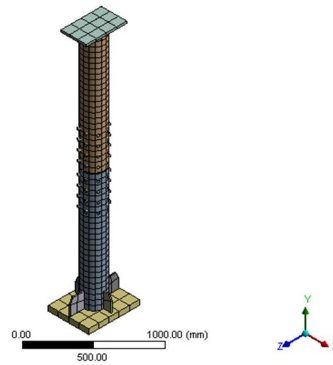


Fig 23:Finite element meshing

A. Cyclic loading

Boundary condition is bottom fixed and top cyclic load applied. Similar to square cross section cyclic loading is applied as per FEMA protocol.

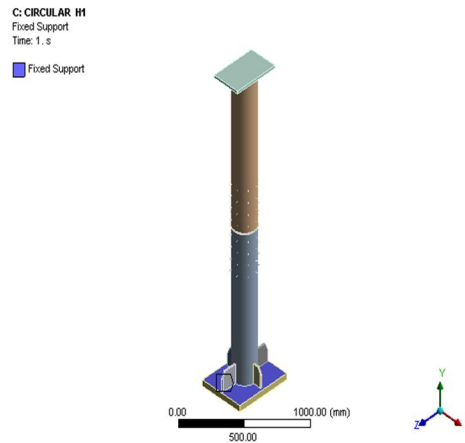


Fig .24. Bottom fixed support

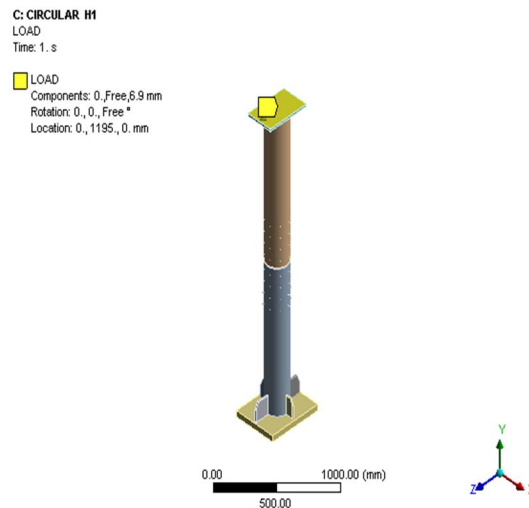


Fig .25. Top cyclic load applied

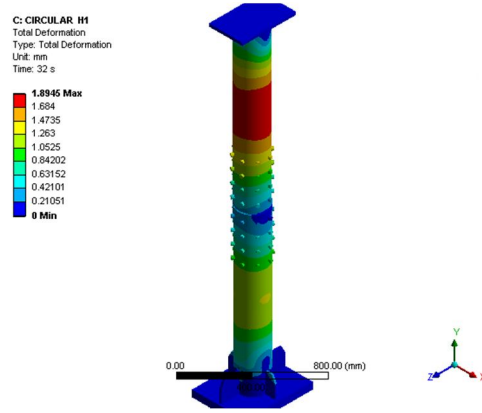


Fig . 26. Total deformation

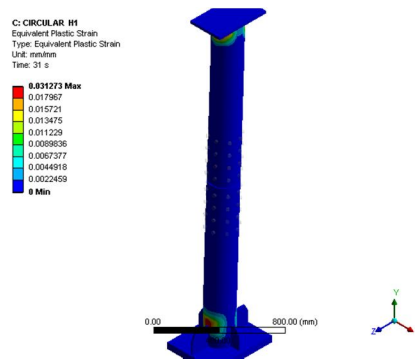


Fig .27. Equivalent plastic strain

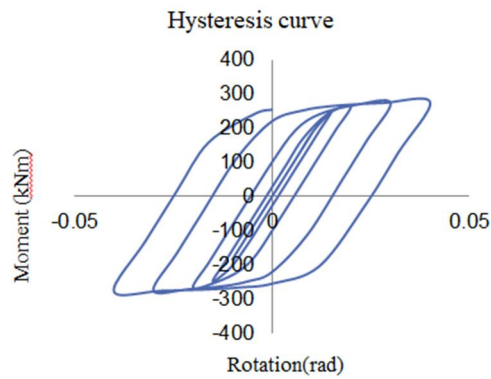


Fig .28. Hysteresis curve obtained after cyclic testing

B. Effect of axial loading by varying thickness of splice plate

Table 9
Cases for varying thickness.

Thickness of splice plate	Designation
14mm	CIRCULAR AL T14
12mm	CIRCULAR AL T12
10mm	CIRCULAR AL T10
8mm	CIRCULAR AL T8
6mm	CIRCULAR AL T6

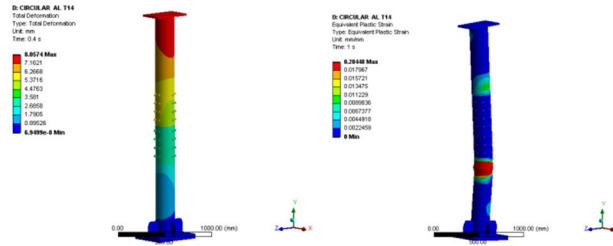


Fig .29. Total deformation and equivalent plastic strain of 14mm splice plate

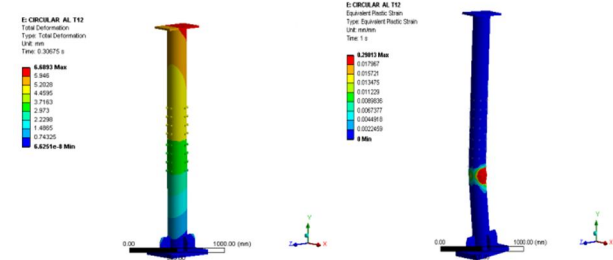


Fig .30. Total deformation and equivalent plastic strain of 12mm splice plate

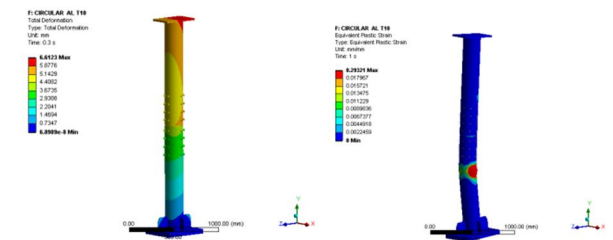


Fig .31. Total deformation and equivalent plastic strain of 10mm splice plate

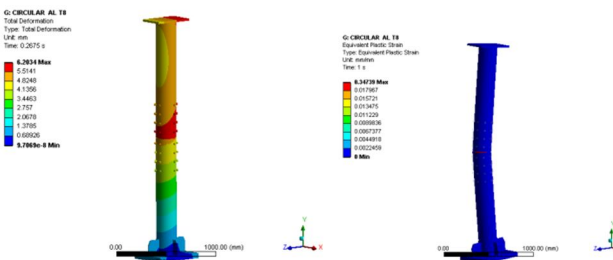


Fig .32. Total deformation and equivalent plastic strain of 8mm splice plate

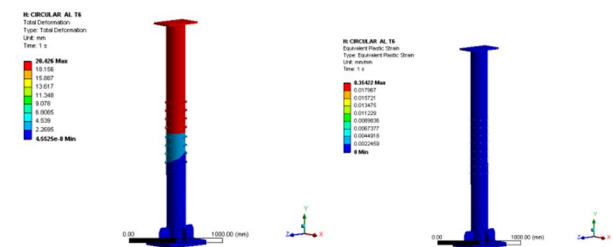


Fig .33. Total deformation and equivalent plastic strain of 6mm splice plate

C. Effect of Axial Loading by varying length of splice plate

Table 10
Cases for varying length.

Length of splice plate	Designation
785mm	CIRCULAR AL 785
685mm	CIRCULAR AL 685
585mm	CIRCULAR AL 585

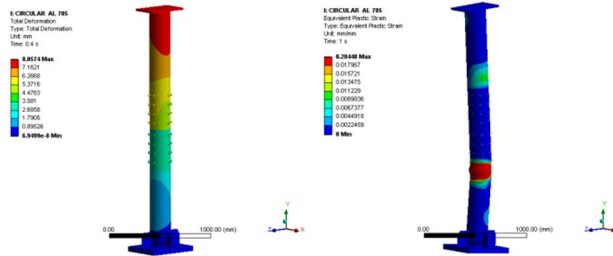


Fig .34. Total deformation and equivalent plastic strain of splice plate of length 785mm

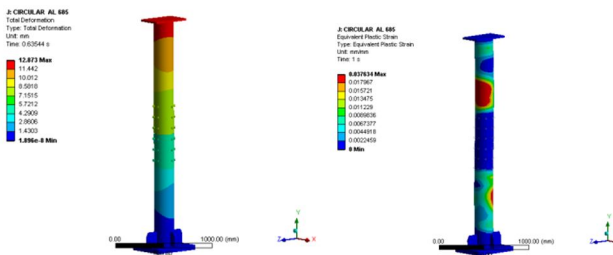


Fig .35. Total deformation and equivalent plastic strain of splice plate of length 685mm

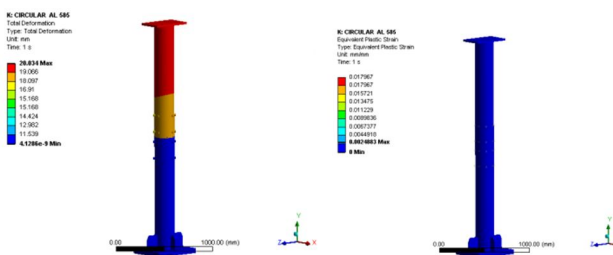


Fig .36. Total deformation and equivalent plastic strain of splice plate of length 585mm

D. Effect of Axial Loading by Varying Diameter of Bolt

Table 11
Cases for varying bolt diameter.

Diameter of bolt	Designation
M24	CIRCULAR AL M24
M22	CIRCULAR AL M22
M20	CIRCULAR AL M20
M18	CIRCULAR AL M18
M16	CIRCULAR AL M16

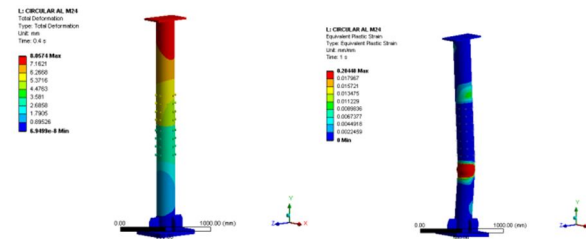


Fig .37. Total deformation and equivalent plastic strain of bolt diameter M24

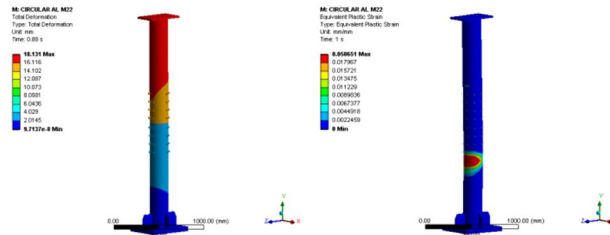


Fig. 38. Total deformation and equivalent plastic strain of bolt diameter M22

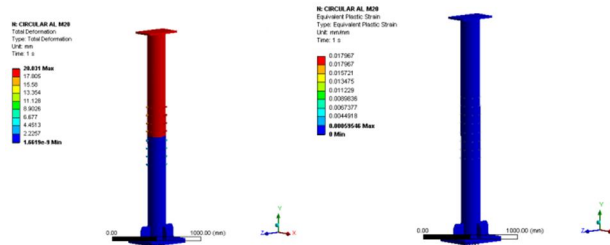


Fig .39. Total deformation and equivalent plastic strain of bolt diameter M20

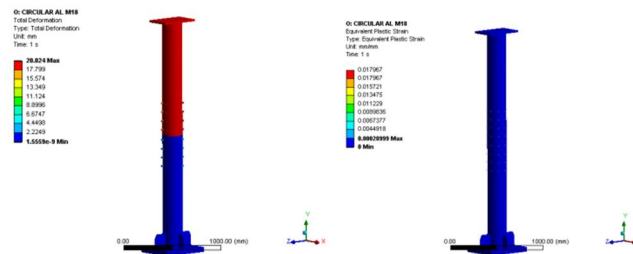


Fig .40. Total deformation and equivalent plastic strain of bolt diameter M18

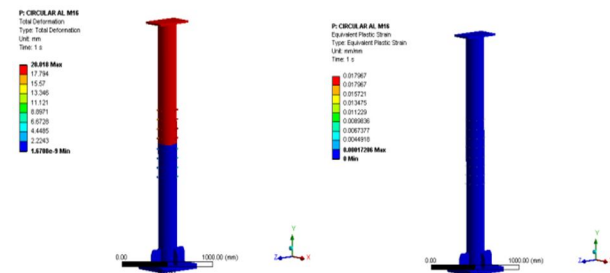


Fig .41. Total deformation and equivalent plastic strain of bolt diameter M16

E. Effect of Axial Loading by Varying bolt Pattern

Table 12
Cases for varying bolt pattern.

Bolt pattern	Designation
64 bolts	CIRCULAR AL 64
48 bolts	CIRCULAR AL 48
32 bolts	CIRCULAR AL 32

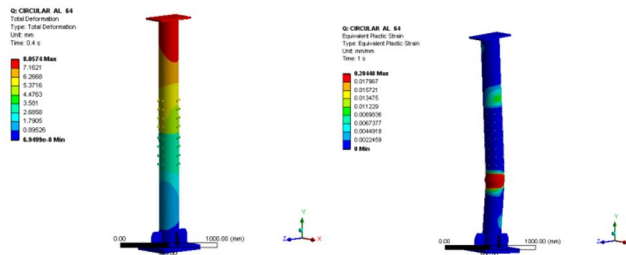


Fig .42. Total deformation and equivalent plastic strain of 64 number of bolts

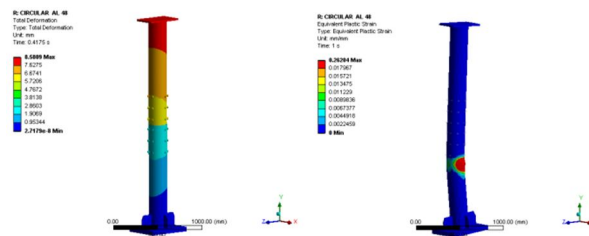


Fig .43. Total deformation and equivalent plastic strain of 48 number of bolts

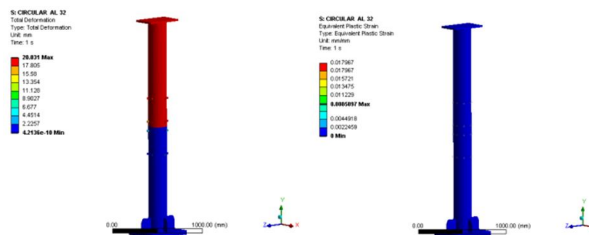


Fig .44. Total and equivalent deformation plastic strain of 32 number of bolts

V. RESULTS

From the analysis carried out using ANSYS WORKBENCH 2022 R2 ultimate load and corresponding deformations were plotted.

A. For Square Cross section

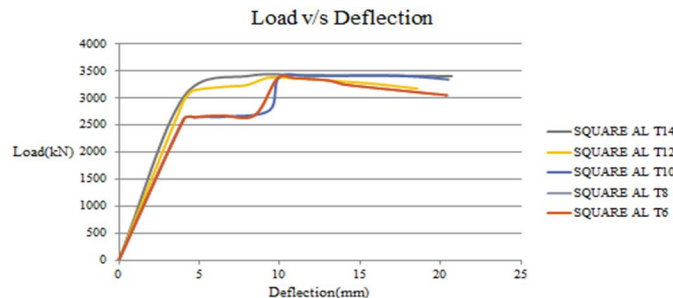


Fig .45. Load v/s Deflection curve for varying splice thickness

Table 13

Ultimate load and ultimate deflection for varying thickness of splice plate.

Splice thickness	Deflection(m m)	Load(k N)	%
SQUARE AL T14	12.06	3412	-
SQUARE AL T12	9.82	3374.1	1.11
SQUARE AL T10	15.55	3407.2	0.14
SQUARE AL T8	10.97	3361.9	1.47
SQUARE AL T6	10.97	3361.9	1.47

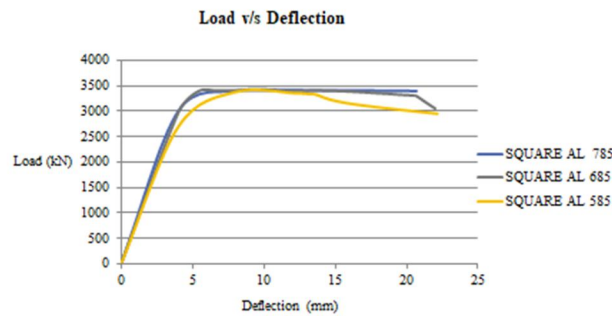


Fig .46.Load v/s Deflection curve for varying splice length

Table 14

Ultimate load and ultimate deflection for varying length of splice plate.

Splice Length	Deflection(mm)	Load(kN)	%
SQUARE AL785	12.057	3412	-
SQUARE AL 685	9.2039	3407.70	0.13
SQUARE AL 585	8.0245	3380	0.94

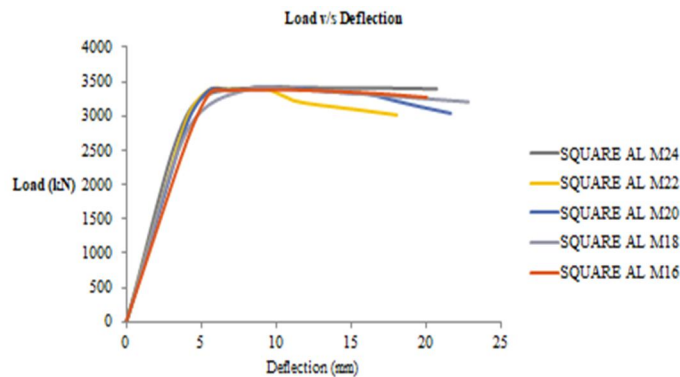


Fig .47. Load v/s Deflection curve for varying bolt diameter

Table 15
Ultimate load and ultimate deflection for varying diameter of bolt.

Bolt Diameter	Deflection(mm)	Load(kN)	%
SQUARE AL M24	12.057	3412	-
SQUARE AL M 22	8.2853	3401.7	0.30
SQUARE AL M 20	11.125	3403.4	0.25
SQUARE AL M18	8.0181	3384.6	0.80
SQUARE AL M16	8.908	3382	0.88

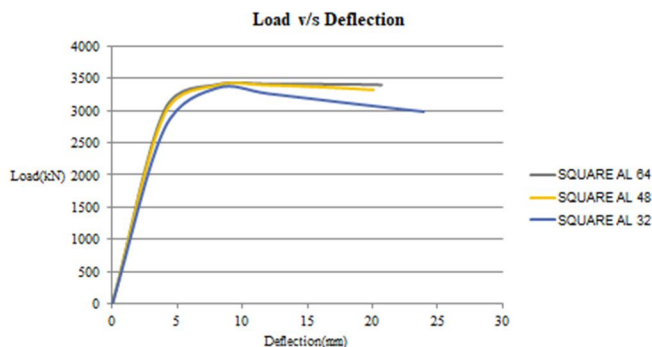


Fig .48. Load v/s Deflection curve for varying bolt pattern

Table 16
Ultimate load and ultimate deflection for varying bolt pattern.

Bolt pattern	Deflection(mm)	Load(kN)	%
SQUARE AL 64	12.057	3412	-
SQUARE AL 48	12.035	3392	0.59
SQUARE AL 32	8.038	3347.1	1.90

B. For Circular Cross Section

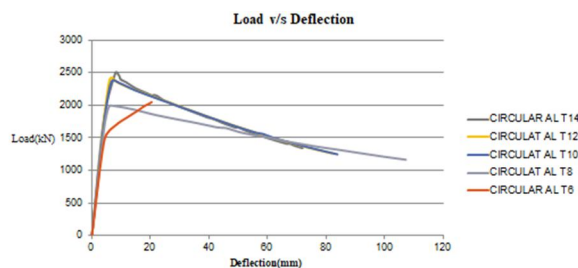


Fig . 49. Load v/s Deflection curve for varying splice thickness

Table 17
Ultimate load and ultimate deflection for varying thickness of splice plate.

Splice thickness	Deflection(mm)	Load(kN)	%
CIRCULAR AL T14	8.0574	2503.5	-
CIRCULAR AL T12	6.6893	2423.4	3.20
CIRCULAR AL T10	6.6123	2357.8	5.82
CIRCULAR AL T8	6.2034	1991.8	20.44
CIRCULAR AL T6	20.426	2048.2	18.19

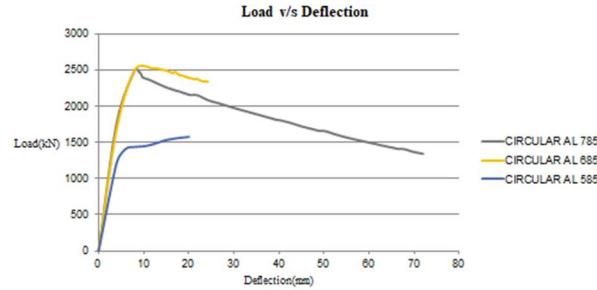


Fig .50. Load v/s Deflection curve for varying splice length

Table 18

Ultimate load and ultimate deflection for varying length of splice plate.

Splice Length	Deflection(mm)	Load(kN)	%
CIRCULAR AL785	8.0574	2503.5	-
CIRCULAR AL 685	12.873	2520.4	0.68
CIRCULAR AL 585	20.034	1575.8	37.06

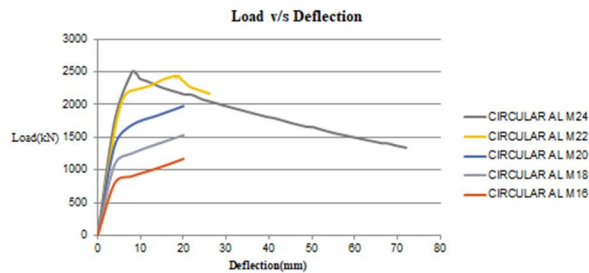


Fig .51. Load v/s Deflection curve for varying bolt diameter

Table 19

Ultimate load and ultimate deflection for varying diameter of bolt.

Bolt Diameter	Deflection(mm)	Load(kN)	%
CIRCULAR AL M24	8.0574	2503.5	-
CIRCULAR AL M 22	18.13	2438.8	2.58
CIRCULAR AL M 20	20.03	1976.6	21.05
CIRCULAR AL M18	20.03	1532.9	38.77
CIRCULAR AL M16	20.02	1170.8	53.23

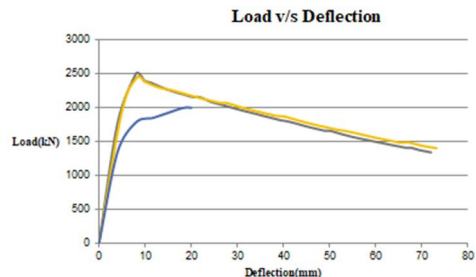


Fig .48. Load v/s Deflection curve for varying bolt pattern

Table 20. Ultimate load and ultimate deflection for varying bolt pattern.

Bolt pattern	Deflection(mm)	Load(kN)	%
CIRCULAR AL 64	8.0574	2503.5	-
CIRCULAR AL 48	8.5809	2455.8	1.91
CIRCULAR AL 32	20.031	1997.1	20.23

VI. INTERPRETATION OF RESULTS

Table 21. Maximum strength case under axial loading

Cross section	Maximum load carrying capacity	Cases
SQUARE	3412kN	14x785XM24x64
CIRCULAR	2520.4kN	14x685XM24x64

VII. CONCLUSION

- 1) Finite element analysis is an effective method to study the behavior of the connections.
- 2) The tubular columns with deconstructable splice connection with maximum load give greater strength. The section with maximum deflection gives greater ductility.
- 3) 3-D finite element models were developed and tested for cyclic loading for circular cross section which showed maximum moment of 277.67kNm with 3% drift.
- 4) For square column cyclic loading test almost gave same results obtained from experiment using Specimen H1 with 0.8% error in moment and storey drift of 2.44. Maximum bending moment of 251.77kNm and storey drift of 4.1 was obtained from software.
- 5) Studied the axial behavior of square and circular steel tubular columns with deconstructable splice joint. Columns showed local buckling in most cases. Square section has maximum load carrying capacity of 3412kN.
- 6) From the parametric study conducted on square and circular cross section of steel tubular column with deconstructable splice joint, we can conclude that variation of splice and bolt parameters affect the strength, stiffness and ductile characteristics of column section. Going beyond materials ultimate strength can result in failure, such as buckling or excessive deformation.

REFERENCES

- [1] Ataei, A., Bradford, M. A., Valipour, H. R., & Liu, X.(2016). Experimental study of sustainable high strength steel flush end plate beam-to-column composite joints with deconstructable bolted shear connectors. *Engineering Structures*, 123, pages 124-140.
- [2] Cai, Y., Quach, W. M., Chen, M. T., & Young, B.(2019) Behavior and design of cold-formed and hot-finished steel elliptical tubular stub columns. *Journal of Constructional Steel Research*, volume 156.
- [3] Chen, M. T., & Young, B.(2019). Material properties and structural behavior of cold-formed steel elliptical hollow section stub columns. *Thin-Walled Structures*, volume 134, pages 111-126.
- [4] Fan, J., Yang, L., Wang, Y., & Ban, H.(2022).Research on seismic behaviour of square steel tubular columns with deconstructable splice joints. *Journal of Constructional Steel Research*, volume 191, pages 107-204.
- [5] Fan, S., Xie, S., Wang, K., Wu, Y., & Liang, D.(2022). Seismic behaviour of novel self-tightening one-side bolted joints of prefabricated steel structures. *Journal of Building Engineering*, volume 56, pages 104-823.
- [6] Liu, X. C., He, X. N., Wang, H. X., & Zhang, A. L.(2018).Compression-bend-shearing performance of column-to-column bolted-flange connections in prefabricated multi-high-rise steel structures. *Engineering Structures*, volume 160, pages 439-460.
- [7] Liu, X. C., Tao, Y. L., Chen, X., & Chen, M. L.(2022).Seismic performance of bolted flange splicing joints for CFST columns. *Journal of Constructional Steel Research*, volume 196, pages 107-412.
- [8] Pongiglione, M., Calderini, C., D'Aniello, M., & Landolfo, R.(2021) Novel reversible seismic-resistant joint for sustainable and deconstructable steel structures. *Journal of Building Engineering*, volume 35.
- [9] Uy, B., Patel, V., Li, D., & Aslani, F.(2017). Behaviour and design of connections for demountable steel and composite structures. In *Structures*, volume 9, pages 1-12
- [10] Wang, W., Li, M., Chen, Y., & Jian, X.(2017) Cyclic behavior of endplate connections to tubular columns with novel slip-critical blind bolts. *Engineering Structures*, volume 148.
- [11] Ye, J., Mojtabaei, S. M., Hajirasouliha, I., & Pilakoutas, K.(2020). Efficient design of cold-formed steel bolted-moment connections for earthquake resistant frames. *Thin-walled structures*, volume 150
- [12] Wang, Y. Q., Zong, L., & Shi, Y. J.(2013) Bending behavior and design model of bolted flange-plate connection. *Journal of Constructional Steel Research*, volume 84, pages1-16.



10.22214/IJRASET



45.98



IMPACT FACTOR:
7.129



IMPACT FACTOR:
7.429



INTERNATIONAL JOURNAL FOR RESEARCH

IN APPLIED SCIENCE & ENGINEERING TECHNOLOGY

Call : 08813907089  (24*7 Support on Whatsapp)